Direct Observation of Mass Transfer at Solid−Liquid Interface by Laser Flash Photolysis of the Interface Probe Molecules

ARTICLE *in* THE JOURNAL OF PHYSICAL CHEMISTRY B · JULY 2000

Impact Factor: 3.3 · DOI: 10.1021/jp001071n

4 AUTHORS, INCLUDING:

Yu-Xiang Weng
Chinese Academy of Sciences
45 PUBLICATIONS **779** CITATIONS

Direct Observation of Mass Transfer at Solid−Liquid Interface by Laser Flash Photolysis of the Interface Probe Molecules

Yu-Xiang Weng,*,† Hong Xiao,‡ Kwok-Chu Chan,‡ and Chi-Ming Che‡

Institute of Physics, Chinese Academy of Sciences, Beijing 100080, China, and Department of Chemistry, The University of Hong Kong, Pokfulam Road, Hong Kong

Received: March 22, 2000; In Final Form: June 6, 2000

Transient absorption signal delayed by a magnitude of 100 μs with respect to the exciting laser shot is observed after UV laser flash photolysis of degassed benzene, acetone, and acetonitrile solutions of an interface probe complex, i.e., gold(I) complex [{Au[P(C_6H_4OMe-p)$_3$]}$_2$-(μ-C≡C)] ([μ-ethynylene-bis{tris(4-methoxyphenyl)-phosphine}gold]). Chemical reactions leading to the transient absorbance change are confirmed to be occurring at the solid−liquid interface, and the delay time is believed to arise from the photogenerated intermediate species in the bulk solution crossing the diffusion layer, which ultimately undergo interfacial reactions resulting in the observed transient absorbance change. The delay time is suggested as a direct measure for the thickness of the diffusion layer. The thickness of the diffusion layer around 0.2 μm, estimated by this method, is comparable to that from the sonovoltammetric study. Oscillations in transient absorbance kinetics are also observed, which can be attributed to the coupling between the interfacial chemical reactions and a photoacoustic effect; oscillation due to a single physical process arising from the schlieren effect under certain condition is also discussed. Similar transient phenomena are observed in another luminescent complex, i.e., a hexanuclear Cu(I) cluster Cu_6(t-NS)$_6$ (t-NS = 4-*tert*-butylpyridine-2-thiolate). The characterization of the photochemical reaction processes of the Cu(I) complex by means of transient absorbance difference spectra reveals that a consecutive biphotonic ionization process occurs after the laser flash. The intermediate species with a lifetime of 65 μs responsible for the interfacial reaction is tentatively assigned as a charge separation pair. A reaction scheme involving surface-assisted ionization of the charge separation pair is proposed to account for the coupling between the interfacial chemical reaction and the photoacoustic effect.

Introduction

Interfacial chemical reactions have attracted intense research interest during the past decades for their relevance to a various important fields, e.g., biological systems,[1] solar energy conversion,[2,3] and photocatalytic process.[4] Generally, any interfacial reaction must involve a mass transfer process from one phase to another. For a fast heterogeneous reaction, the interfacial mass transfer process can be a rate-determining step, which affects the total reaction efficiency. Taking a solid−liquid interface as an example, mass transfer crossing the diffusion layer is the main barrier for the efficient mass transport. Study on the efficiency of mass transfer, hence the average thickness of the diffusion layer under various conditions, is still of current interest in electrochemistry,[5,6] where the thickness of a diffusion layer can be inferred from the mass-transport limiting current at the electrode with a method of rotating disk electrode[7,8] or sonovoltammetry.[9,10] Very recently, Amatore et al. published a series of papers on direct mapping of the concentration profiles within the diffusion layer by means of confocal resonance Raman spectra,[11] potentiometric measurement,[12] and amperometric measurement[13] with an ultramicroelectrode probe.

In this paper, we report an interfacial probe molecule [{Au[P(C_6H_4OMe-p)$_3$]}$_2$-(μ-C≡C)], which can generate active intermediate species capable of undergoing interfacial chemical reaction and indicates the start of an interfacial process when subjected to UV laser flash photolysis. By measuring the time difference between the laser shot and the onset of the interfacial process, the migration time for the laser-generated intermediate species crossing from the bulk to the interface is obtained. The diffusion layer thickness which, equals the migration time multiplied by the migration velocity, can be estimated once the migration rate of the intermediate species is known, providing a straightforward way for determining the diffusion layer thickness. That this direct method is feasible is mainly because of the rare photochemical properties of the title complex. However, due to the photodecomposition of the Au(I) complex, the photochemical reaction, as well as the subsequent interfacial chemical reactions, can hardly be well understood. Fortunately, in our effort to search for new compounds having the same function, we found that similar transient phenomena can be regenerated in a less photolabile complex, i.e., Cu_6(t-NS)$_6$ (t-NS = 4-*tert*-butylpyridine-2-thiolate). The relative stability of the Cu(I) complex under laser photolysis points an entry to the study of the reaction mechanism. The photochemical reaction of the Cu(I) complex is confirmed to be a biphotonic ionization process, giving rise to an intermediate species presumably assigned as a charge separation pair characterized by transient absorption spectra. The interfacial process is suggested as an interface-assisted ionization of the charge separation pair.

When a pulsed laser is employed as the excitation source, photoacoustic effect can be invoked in the flash photolysis

* To whom correspondence should be addressed. Tel: (8610)-82649342. Fax: (8610)-82649531. E-mail:yxweng@aphy.iphy.ac.cn.
† Chinese Academy of Sciences.
‡ The University of Hong Kong.

10.1021/jp001071n CCC: $19.00
Published on Web 07/26/2000

experiment. As reported in our previous work, laser-generated ultrasonic reflection between the two parallel cell walls can be coupled to chemical reactions and modulates the transient absorption signal leading to a series oscillation peaks on the kinetic trace.[14] Herein we also report observations of the similar ultrasonic reflection signal under certain conditions in neat solvents generated by a single physical process, thus it is important to distinguish whether the observed ultrasonic reflection signal originates from a chemical or a physical process. Identification and discussion of the chemical- and physical-based oscillations are presented.

Experimental Section

Preparation. All chemicals used in syntheses were reagent grade and used without further purification. Solvents for spectroscopic and photochemical studies were redistilled before use. The ligand t-NSH (4-*tert*-butylpyridine-2-thiol) was prepared in this laboratory. The complex Cu_6(t-NS)$_6$ was prepared according to a modified literature method for the related hexanuclear copper (I) thiolates.[15−17] The Cu(I) complex was characterized by elemental analysis: calculated ratios (%) of elements in $Cu_6(C_9H_{12}NS)_6$ are C, 47.04; H, 5.26; N, 6.09. Experimental found ratios were C, 48.01; H, 5.29; N, 6.08. The complex [{Au[P(C_6H_4OMe-p)$_3$]}$_2$-(μ-C≡C)] was prepared according to the literature method.[18−19]

Instrumentation. The UV−visible absorption spectra were recorded on a Perkin-Elmer Lambda 19 spectrophotometer, and the steady-state emission spectra on a SPEX Fluorolog-2 spectrophotometer. The time-resolved absorption signals were measured on a conventional flash photolysis setup described elsewhere.[14,20] Briefly, the flash photolysis setup consists of the 355 nm output of a Quanta-Ray DCR-3 with Nd:YAG laser (fwhm = 8 ns) as the excitation beam. The monitoring light was from a 300 W cw Xenon−halogen lamp having a beam profile of ca. 1 cm in diameter. The defocused excitation beam with a diameter of ca. 1 cm was directed onto an absorption cuvette. Unless otherwise specified, the excitation and probe beams were arranged in a normal configuration. The probe beam was detected by a six-stage R928 photomultiplier tube (PMT). The transient absorption signals were amplified and recorded on a digital storage oscilloscope interfaced to a computer for data transfer. All solutions were degassed by four freeze−pump−thaw cycles prior to measurement, and the experiments were performed at room temperature (24 ± 2 °C).

Results

The photochemical and photophysical properties of the complex [{Au[P(C_6H_4OMe-p)$_3$]}$_2$-(μ-C≡C)] have been reported elsewhere.[19] The excited emissive state has a lifetime about 4.0 μs in a degassed dichloromethane solution. When subjected to the flash photolysis, the complex exhibits a transient absorbance decay trace of unusual features as shown in Figure 1. Figure 1a shows the transient absorption signal acquired in a benzene solution of Au(I) complex probed at 580 nm, displaying a delayed oscillation signal. Similar transient absorption traces were found appearing in the whole accessible spectral region (380 nm to 760 nm); the kinetics were probed at 580 nm unless otherwise notified. The selection of this wavelength is based on the consideration of a better signal-to-noise ratio. Control experiments were conducted in a clean cell filled with the same solvent, or even filled with a light-absorbing medium such as Rhodamine 6G doped solvent ($c \approx 10^{-4}$ M, $\epsilon_{355} \approx 1.1 \times 10^4$ mol^{-1}dm^{3}cm^{-1} in methanol), no transient absorption signal was observed. When the coupling between a chemical reaction and ultrasonic reflections is present, the transient kinetic trace appears in a form shown in Figure 1b, where the first phase immediately after the laser shot has a series of oscillation peaks riding on a decaying envelop, followed by a delayed oscillation signal similar to Figure 1a. The observation and a preliminary explanation of the oscillatory phenomenon in the first phase has been given in our previous work,[14] and this oscillation is attributed to the coupling of the photochemical reaction with reflected ultrasonic waves, resulting in a series of peaks in a transient absorption decay trace with temporal spacing being the time interval for the ultrasonic waves to travel between the two parallel cell walls.

A distinct feature of the transient signal in Figure 1 is that the absorption signal (in Figure 1b the delayed phase is referred) appears after a delay time of about 100 μs after the laser pulse. Further experiments reveal that this delay time depends on the laser intensity (Figure 1b inset) and the filled liquid volume in the cell (Figure 2). As shown in the inset in Figure 1b, at the fixed liquid volume and when the laser power exceeds 15 mJ/pulse, the delay time decreases with the increase of excitation power. The dependence of the delay time on the excitation power can be described roughly by a linear relation as shown by the solid line in the graphic inset. On the other hand, it is found that the delay time increases with the filled liquid volume in the sample cell at the fixed laser power. Figure 2 shows the linear dependence of the delay time on the filled liquid height in two cells of different geometry, i.e., 1.0 × 1.0 cm and 1.0 × 2.0 cm, where the excitation path lengths were kept at 1.0 cm. The slopes of the two linear fitting are 5.84 (for 1.0 × 2.0 cm cell) and 2.42 (for 1.0 × 1.0 cm cell), respectively. If the delay time is linearly proportional to the liquid volume, the expected ratio for the two slopes would be 2.0, and the observed value is 2.4; furthermore, at the same liquid volume, the observed delay times in the two different cells are quite close, which also concludes that the delay time depends on the liquid volume. The two intercepts obtained from linear fitting of the experimental data do not equal zero, they are 2.9 ± 12.9 μs for the 1.0 × 2.0 cm cell and 4.9 ± 1.7 μs for the 1.0 × 1.0 cm cell. In addition to the above two controlling parameters (laser power and the filled liquid height), we also investigated the effect of distance between the excitation beam and the cell wall being probed on the delay time in a 1.0 × 1.0 cm cell filled with a 9.0 × 10^{-5} M acetone solution of Au(I) complex, where the excitation beam was parallel to the cell walls being probed. The excitation beam size was reduced to a spot with a diameter of ca. 4 mm by using a convex lens. At fixed excitation power and fixed filled liquid volume, it is found that the delay times remain unchanged, regardless of whether the probe beam is centered, right-, or left-displaced from the center of the cell.

After prolonged flash photolysis, two dark gray spots developed on the inner surface of the two cell walls where the excitation laser beam impinged on the sample cell. The deposited metallic film indicates that a photochemical reaction occurred at the solid−liquid interface, leaving the metallic gold as the product. The metallic film deposition on the cell wall due to the laser flash photolysis suggests that the chemical reaction can be an interfacial process. To examine whether the excitation laser induces any interfacial chemical reactions, the solution was transferred from the cuvette to the degassing flask,[14] leaving only a liquid film coating on the inner surface of the cuvette. The excitation and probe beams were arranged so as to be overlapping at the two interfaces being probed. Figure 3 shows the transient absorption decay traces recorded for the liquid film when the excitation and probe beams overlap. There are three

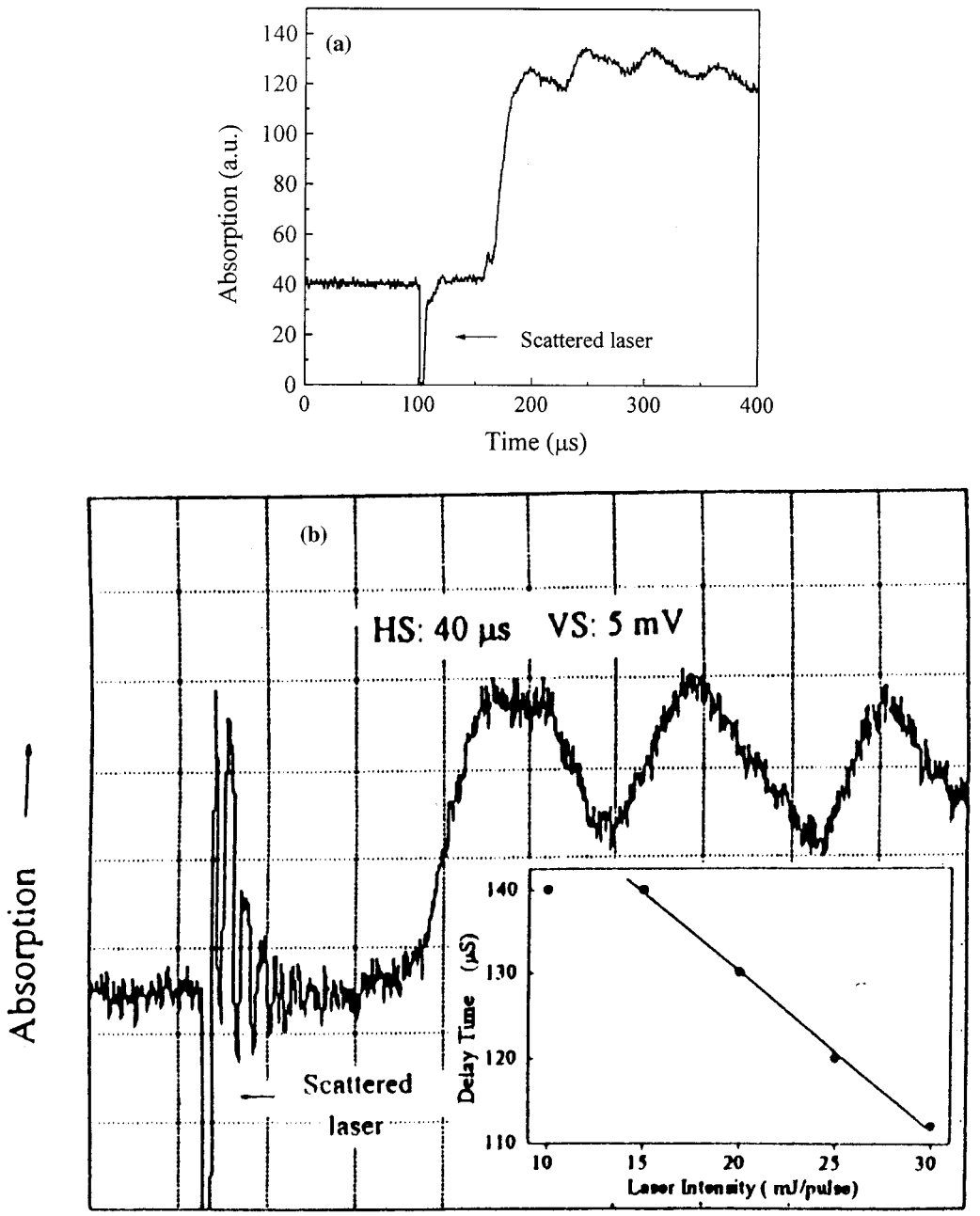

Figure 1. Oscillograms showing delayed oscillatory transient absorption signals for a degassed benzene solution of $[\{Au[P(C_6H_4OMe\text{-}p)_3]\}_2\text{-}(\mu\text{-}C{\equiv}C)]$ in a 1.0 × 1.0 cm cell probed at 580 nm. (a) Without the presence of the laser-generated ultrasonic reflection, $c = 2.8 \times 10^{-4}$ M; laser intensity: 24 mJ/pusle. (b) With the presence of the laser-generated ultrasonic reflection recorded for $c = 1.9 \times 10^{-4}$ M, laser intensity: 25 mJ/pusle; HS: horizontal scale (per division); VS: vertical scale (per division). Graphic inset: plot of the delay time for the onset of the delayed phase against the laser intensity.

traces presented in Figure 3: trace 1 was recorded immediately after the removal of the bulk solution, trace 2 was acquired about 5 min after the acquisition of trace 1, and trace 3 is the subtraction of trace 2 from trace 1. Trace 1 shows a biphasic kinetic process, whereas trace 2 exhibits only a monotonical decay. The only difference between trace 1 and trace 2 is that the film in the former is thicker than in the latter. These two kinetic traces can possibly reveal the dynamic process at different layers of a solid−liquid interface that consists of an adsorbed layer and a liquid continuum.

A limiting case of gradual increase in the thickness of the liquid film would be the bulk solution, where the liquid film finally becomes the bulk solution. Figure 4a shows a transient absorption signal for the bulk solution where the excitation and probe beams overlap each other at the interfaces being probed. Figure 4b is an expanded view of the early kinetics. Compared to the kinetic trace 1 for a thin liquid film in Figure 3, the feature at the early time (Figure 4b) is quite similar; however, a new peak at 210 μs similar to the delayed kinetic phase in Figure 1a indicates a feature unique to the bulk solution.

To further confirm that the undergoing chemical reaction is an interfacially related process, flash photolyses of the solution complex were carried out in cells of the same geometry, but made of different materials (Figure 5), i.e., a glass and a quartz cell, respectively. The results show that the kinetic trace decays faster in the glass cell than in the quartz. The fact also suggests that the chemical reaction in question occurs at the solid−liquid interface rather than in the bulk solution. In addition to the interfacial characteristics of the photochemical reactions, a remarkable feature is that the photochemical process can be

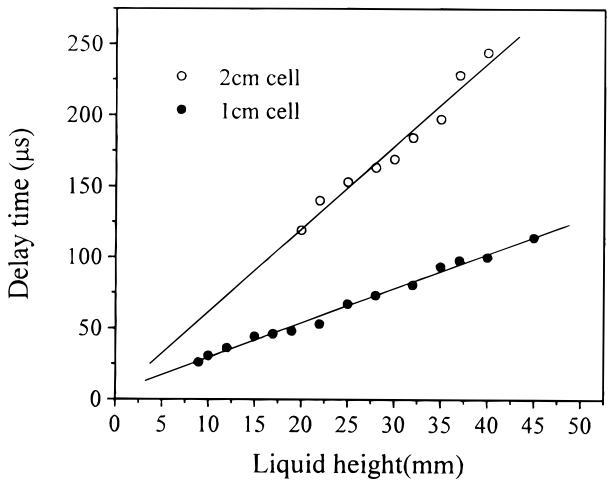

Figure 2. Dependence of the delay time on the filled liquid height observed for a 9.0×10^{-5} M acetone solution of the complex [{Au-[P(C_6H_4OMe-p)$_3$]}$_2$-(μ-C≡C)] in a 1.0 × 1.0 cm and a 2.0 × 1.0 cm quartz cell respectively, probed at 580 nm. Laser intensity: 15 mJ/pulse.

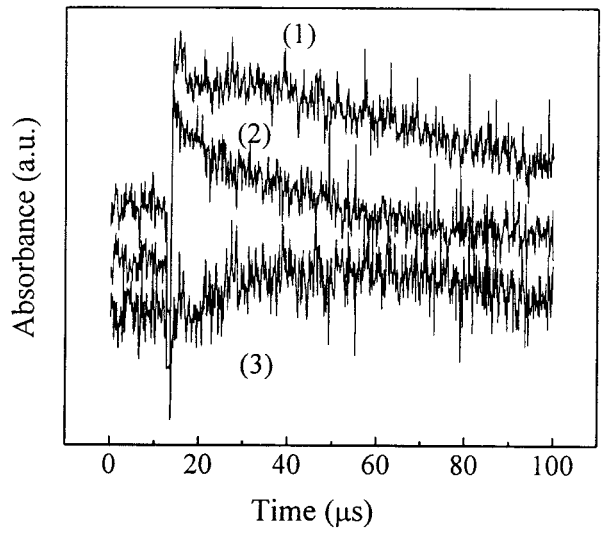

Figure 3. Transient absorption signals for the liquid film on the inner surface of the cell, acquired at a single laser shot. Trace 1 acquired immediately after the removal of the solution; trace 2 acquired about 5 min after the acquisition of trace 1; trace 3 is the difference between trace 1 and trace 2. Laser intensity: 15 mJ/pulse, probed at 580 nm. The excitation and probe beams were arranged in an overlapping fashion.

quenched upon inlet of the dioxygen into the degassing cell, as indicated by the flat kinetics (dotted line) shown in Figure 6, which exclusively precludes the possibility that the transient signal originates from a single physical process or malfunction of the instruments. Since the excited-triplet state of the Au(I) complex has a lifetime about 4.0 μs, which would be quenched by dioxygen, the fact suggests that the underlying photochemical process is an excited-triplet state related chemical process. The excited-triplet state of the Au(I) complex may undergo photoionization or further decomposition upon absorption of an extra photon. Our trial to acquire a transient absorption spectrum of the Au(I) complex failed due to the photodecomposition of the Au(I) complex, which formed a metallic film on the cell wall and gave rise to an intense photoacoustic effect. This effect is found to be a severe interfering factor in quantitative measurement of the transient absorbance, preventing the acquisition of

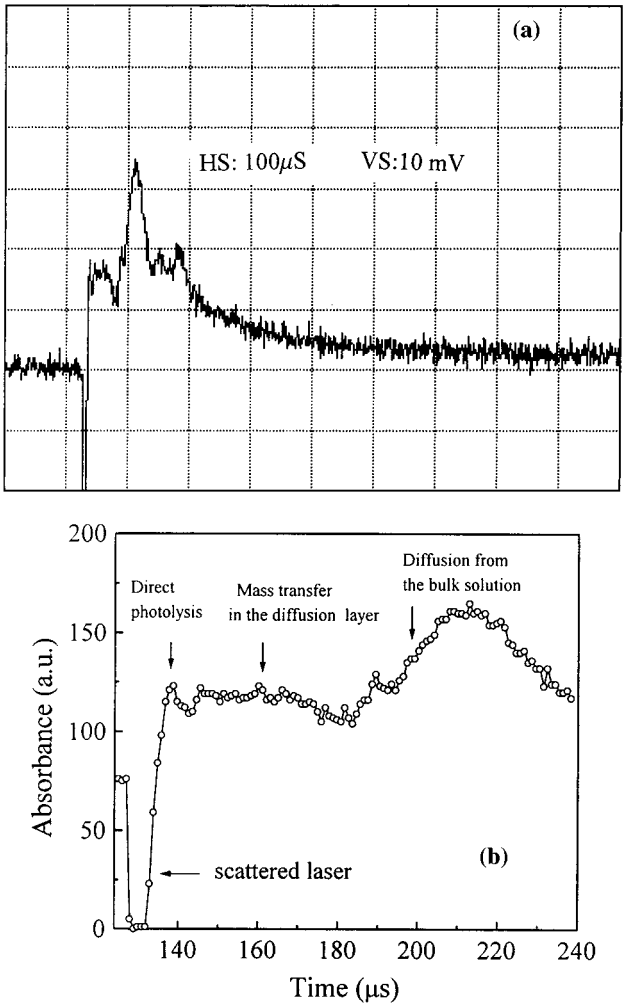

Figure 4. Transient absorption signals acquired for the bulk solution with an overlapping configuration between the excitation and probe beams in a degassed benzene solution of [{Au[P(C_6H_4OMe-p)$_3$]}$_2$-(μ-C≡C)], $c = 2.8 \times 10^{-4}$ M, laser intensity: 15 mJ/pulse, probed at 580 nm. (a) Viewed at full time scale. (b) Expanded view of the early kinetic trace.

a transient absorption spectrum. This metallic film enhanced photoacoustic effect will be further discussed in a later section.

When the laser beam passed the cell with black spots, the intense photoacoustic effect evoked by metallic film acted as a sound source after absorbing the excitation light. In addition to the reported oscillation phenomenon in a clean cell,[14] our present work reveals that a single physical process, i.e., the metallic film enhanced photoacoustic effect in the neat solvent arising from the light absorption of the metallic film, can also generate the similar oscillations of ultrasonic reflection shown in the first phase of Figure 1b. It is found that these two kinds of oscillations, though appearing in an almost the same waveform in a square cell (1.0 × 1.0 cm), can be discriminated by their oscillation frequency dependence on either probe path length or pump path length by changing the geometry of the cell, e.g., from a square cell to a rectangular one. It has been shown that the oscillation frequency for the coupling between the photoacoustic effect and the photoinduced chemical reaction in the solution of Au(I) complex depends inversely on the path length of the probe beam.[14] In the present work it is found that the oscillation frequency due to the metallic film enhanced photoacoustic in the neat solvents depends inversely only on the excitation path length. We demonstrated this in three cells of different geometry predeposited with metallic film, i.e., 2.0 ×

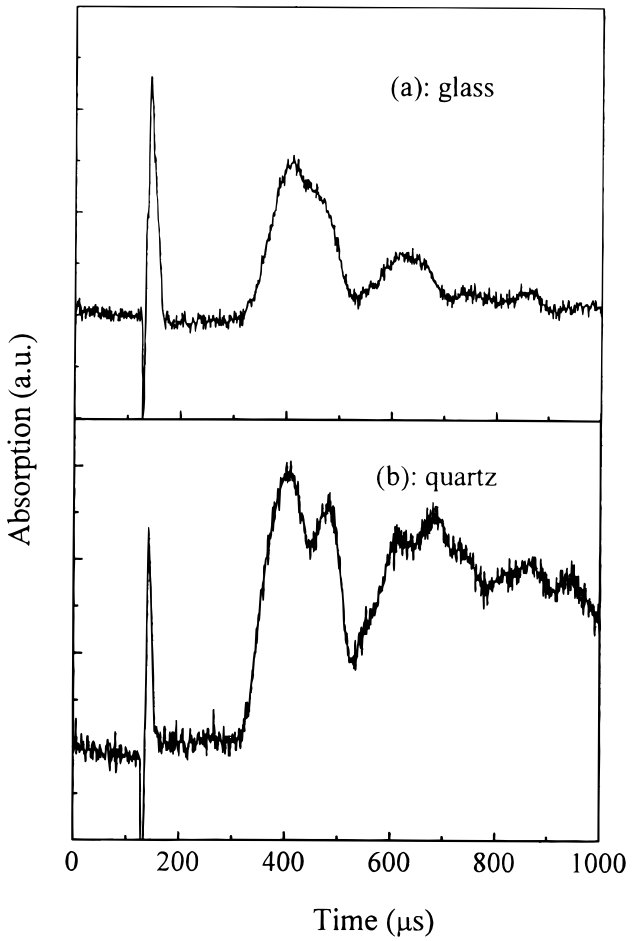

Figure 5. Comparison of oscillograms for flash photolysis of a 6.8×10^{-5} M degassed acetone solution of the complex $[\{Au[P(C_6H_4OMe\text{-}p)_3]\}_2\text{-}(\mu\text{-}C{\equiv}C)]$ in 2.0×1.0 cm degassing cells of different materials: (a) glass; (b) quartz. Excitation path length: 1.0 cm, filled liquid volume: 9.0 mL, laser intensity: 15 mJ/pulse, probed at 580 nm.

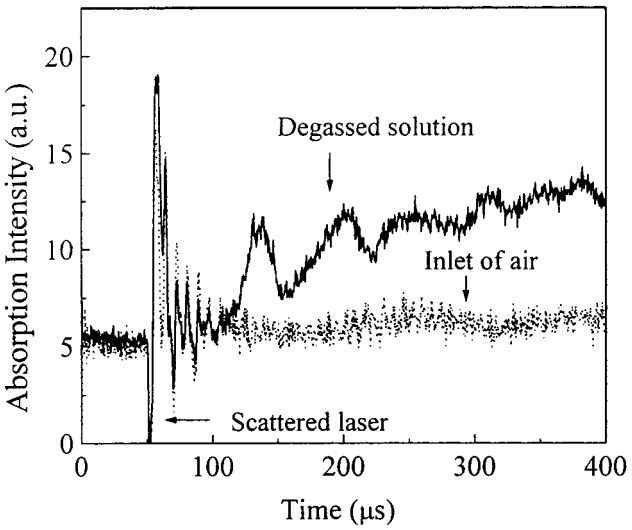

Figure 6. Oscillograms acquired after flashing a 6.8×10^{-5} M acetone solution of the complex $[\{Au[P(C_6H_4OMe\text{-}p)_3]\}_2\text{-}(\mu\text{-}C{\equiv}C)]$ showing that the delayed phase is sensitive to dioxygen. Solid line: degassed sample, dashed line: after the inlet of air. Laser intensity: 15 mJ/pulse, probed at 580 nm.

1.0, 1.0×1.0, and 1.0×0.5 cm filled with acetone, respectively. The predeposited film was achieved by deliberately prolonged laser flash photolysis of the Au(I) complex solution.

TABLE 1: Correlation between FFT Oscillation Frequency of the Laser-Generated Ultrasonic Reflection and the Excitation Path Length in the Film-Enhanced Acoustic Effect Conducted in a Cell Predeposited with a Metallic Film on the Inner Surface Filled of Neat Acetone at a Fixed Probe Path Length of 1.0 cm

excitation path length (cm)	0.5	1.0	2.0
FFT frequency(Hz)	2.4×10^5	1.2×10^5	6.0×10^4

When the probe path length varies from 2.0, 1.0, to 0.5 cm, the oscillation frequency shows no change; while altering the excitation path length in a same way, the oscillation frequency changes in such a way that increasing the excitation path length by a factor of 2, reduces the oscillation frequency to half its value. The results are listed in Table 1.

Though the Au(I) complex acts as a good indicator for an interfacial reaction process, the ongoing photochemical reaction is not well understood. In our effort to search for the new complex acting as an interfacial probe molecule, it is found that $Cu_6(t\text{-}NS)_6$ can also generate a similar transient absorption kinetic trace as the Au(I) complex during flash photolysis. However, the oscillation occurs at a much higher laser intensity (30 mJ/pulse), and no observable metallic film deposition was formed after prolonged flash photolysis, which indicates that the Cu(I) complex is more stable when subjected to the 355 nm laser photolysis. When the employed laser power exceeds 30 mJ/pulse, significant coupling between the photochemical reaction and the acoustic effect occurs. Figure 7 displays the early kinetic phase which consists of a series of oscillation peaks acquired in a 1.0×1.0 cm cell; the graphic inset presents the FFT frequency distribution of the oscillation showing a dominant oscillation frequency of 1.30×10^5 Hz corresponding to the laser generated ultrasonic waves travelling between two parallel cell walls at a separation of 1.0 cm filled with acetonitrile.[14] Trace (a) in Figure 8 depicts the oscillation kinetic trace acquired in a degassed solution and shows the delayed phase appearing at ca. 50 μs after the laser shot. Since the onset of the delayed phase is not well defined owing to a nonzero absorption envelope, the features of the delayed phase were further examined by the dioxygen quenching and the delay time dependence on the filled liquid volume. It is found that the delayed phase can also be quenched by inlet of dioxygen into the degassing cell (trace (b) in Figure 8). Figure 9 describes the linear dependence of the delay time defined by the time difference between the laser shot and the peak position of the delayed phase on the filled liquid height in a 1.0×1.0 cm cell. The linear fitting of the experimental data gives a slope of 2.16 $\pm$ 0.04 and an intercept of 10.9 $\pm$ 1.2 μs. Figure 10 shows the relation between the maximum transient absorption intensity of the delayed phase and the corresponding delay time for the Cu(I) complex (open circle) obtained by varying the filled liquid volume at the fixed laser intensity, which reports the decay of the intermediate species responsible for the observed transient absorbance. The solid line through the data point is the calculated curve of a monoexponential decay with a time constant of 65.4 μs.

Attempts to detect the direct interfacial process using the overlapping configuration of the excitation and probe beams similar to that for Au(I) complex shown in Figure 3 in a liquid film failed. A possible reason can be that the Cu(I) complex is more stable, and a direct photolysis at the solid−liquid interface may not be detectable. Upon excitation with UV light, the complex $Cu_6(t\text{-}NS)_6$ shows an emission maximizing at 760 nm with a lifetime of 3.3 μs at room temperature in a degassed acetonitrile solution. The UV−visible absorption spectrum of

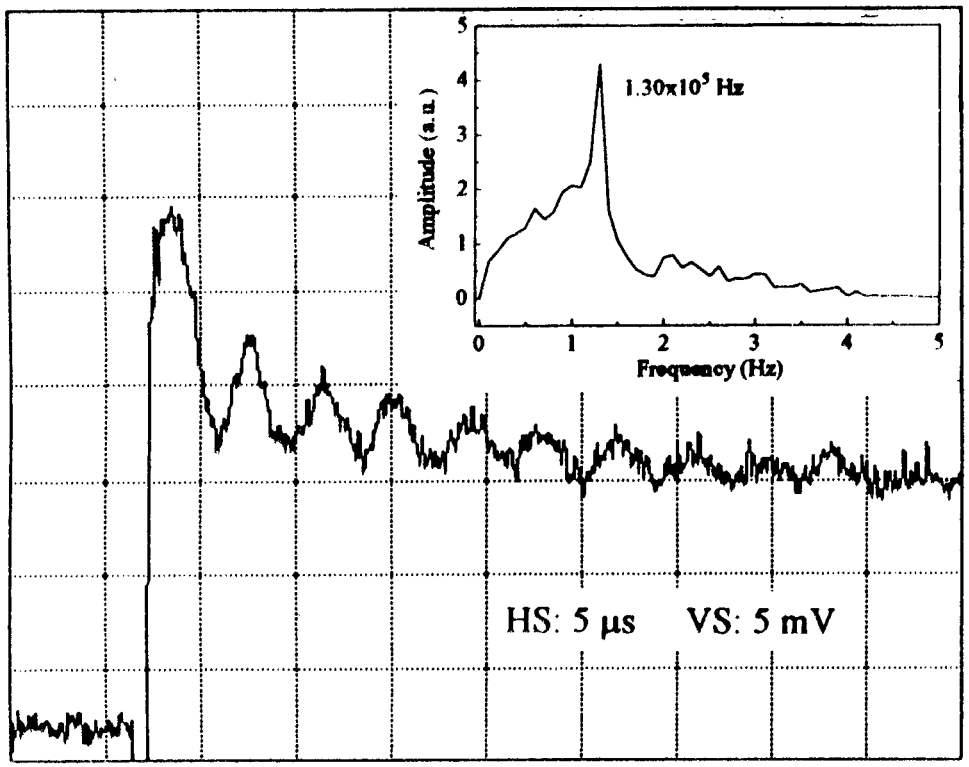

Figure 7. Oscillogram showing the transient oscillations observed in a degassed acetonitrile solution of the complex $Cu_6(t\text{-}NS)_6$ coupled to the laser-generated ultrasonic reflection, $c = 1.0 \times 10^{-4}$ M, laser intensity 37 mJ/pulse probed at 500 nm in a 1.0 × 1.0 cm cell, HS: horizontal scale per division, VS: vertical scale per division. Graphic inset: frequency distribution obtained by FFT analysis.

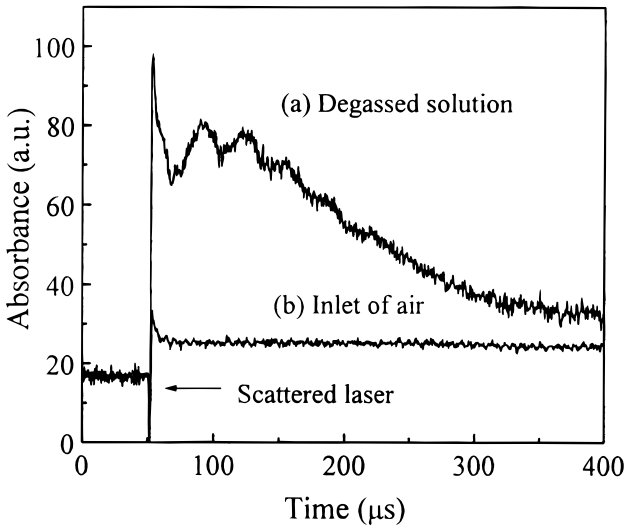

Figure 8. Oscillograms showing the delayed oscillation phase for a degassed acetonitrile solution of the complex $Cu_6(t\text{-}NS)_6$, (trace (a)) and the dioxygen quenching of the oscillation (trace (b)). $c = 9.1 \times 10^{-5}$ M, filled liquid volume: 1.2 mL, laser intensity: 37 mJ/pulse, probed at 500 nm in a 1.0 × 1.0 cm quartz cell.

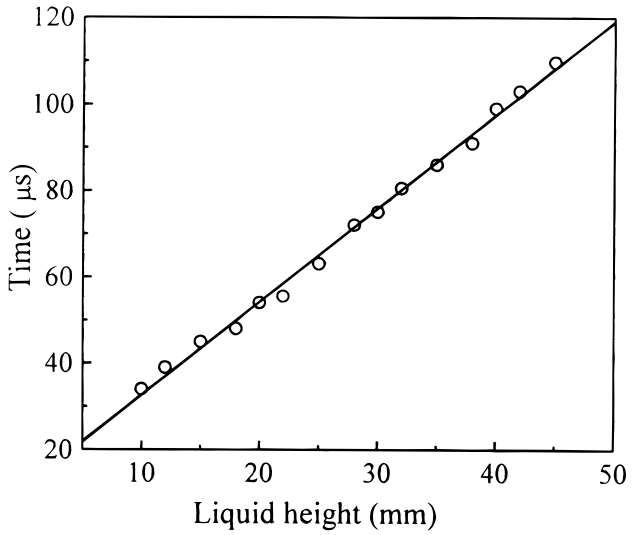

Figure 9. The diffusion delay time dependence on the filled liquid height observed for a 9.1×10^{-5} M acetonitrile solution of the complex $Cu_6(t\text{-}NS)_6$ in a 1.0 × 1.0 cm cell, probed at 500 nm, laser intensity: 37 mJ/pulse.

the complex in acetonitrile is shown in Figure 11, while the luminescence spectrum of the complex solution is given in the graphic inset. Figure 12 shows a typical oscillogram acquired at 400 nm after the laser flash. Two distinct stages of the transient decay were observed after excitation. The fast component can be assigned to the excited-triplet state absorption, for its decay lifetime is 3.3 μs, the same value as that of the luminescence lifetime. However, the absorption signal does not decay to the baseline at a longer time scale; instead, there is a slow decay component having a half-time estimated to be 1.2 ms. Figure 13 depicts the time-resolved absorption difference spectrum of the slow decay component, showing three absorption maxima located at 400, 460, and 800 nm. For comparison, the excited-triplet state absorption spectrum is shown in the graphic inset. It is noted that the decay of the slow component monitored at 400 nm is also biphasic, shown in Figure 14, while the absorption peaks at 460 and 800 nm comprise only a single decay phase which can be fitted by second-order decay kinetics. It was found that the slower decay phase monitored at 400 nm is comparable to the single decay phase monitored at the other two absorption maxima of 460 and 800 nm. When the monitoring wavelength was tuned to 720 nm, the single phase decay trace at 720 nm almost exactly matched the slower decay

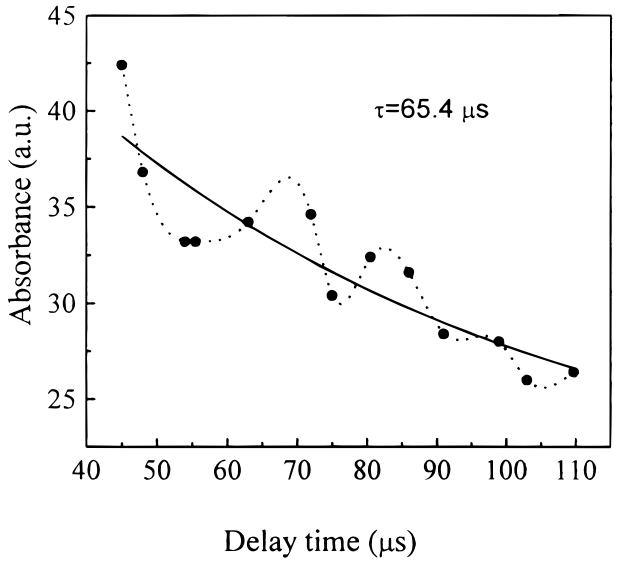

Figure 10. Peak absorption intensity of the delayed phase against the delay time for a degassed 9.1×10^{-5} M acetonitrile solution of Cu_6-(t-NS)$_6$ recorded in a 1.0 × 1.0 cm cell, probed at 500 nm, laser intensity: 37 mJ/pulse. "•": experimental data; the solid line is the calculated single-exponential decay curve with a decay lifetime of 65.4 μs. The dotted line connects the experimental data in a spline way.

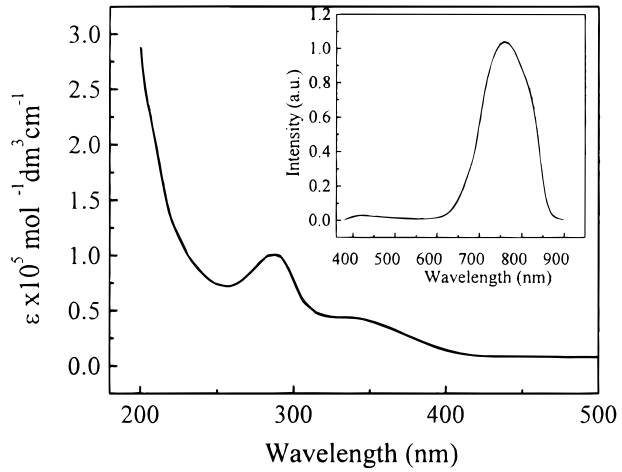

Figure 11. UV−visible absorption spectrum of the complex Cu_6(t-NS)$_6$ in acetonitrile, $c = 2.0 \times 10^{-5}$ M. Graphic inset: luminescence spectrum of the same sample.

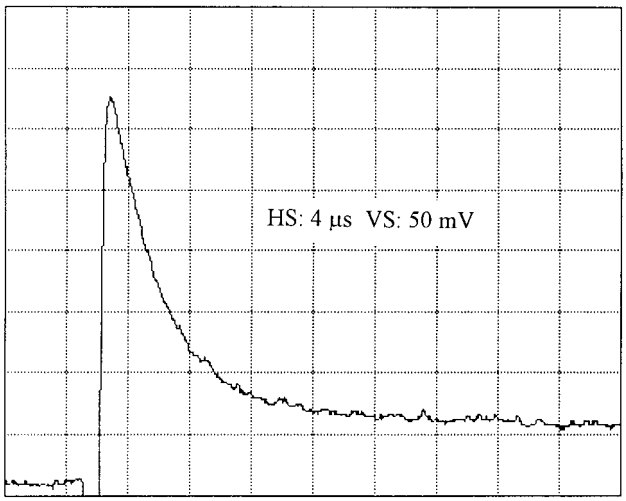

Figure 12. Oscillogram of a typical transient absorption kinetic trace for flash photolysis of a 1.0×10^{-4} M degassed acetonitrile solution of the complex Cu_6(t-NS)$_6$, showing the residual component after the completion of the triplet-state decay probed at 400 nm. Laser intensity: 25 mJ/pulse, HS: horizontal scale per division, VS: vertical scale per division.

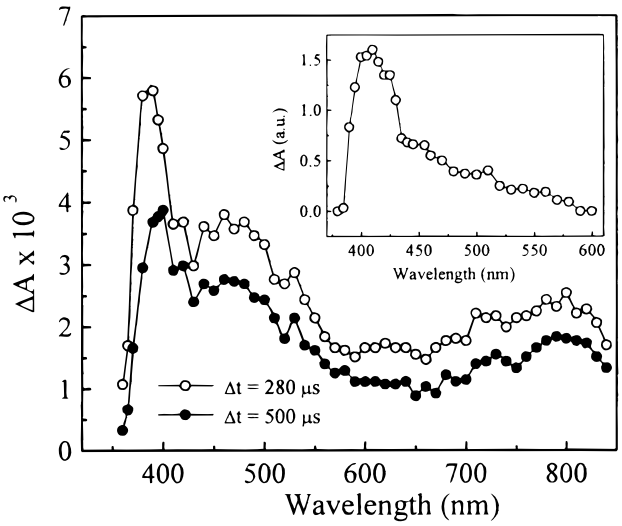

Figure 13. Time-resolved difference absorption spectra of the slow decay component for a degassed acetonitrile solution of the complex Cu_6(t-NS)$_6$, $c = 5.0 \times 10^{-5}$ M, laser intensity: 8 mJ/pulse. Graphic inset: triplet−triplet absorption spectrum of the solution acquired about 1 μs after the laser flash.

component monitored at 400 nm, and thus is plotted for comparison as shown in Figure 14. The graphic inset is the resolved faster decay component monitored at 400 nm having a lifetime of 65.0 μs, obtained by subtraction of the decay trace monitored at 720 nm from that at 400 nm. The relation between the intensity of the transient absorbance change and the excitation laser power was explored for both the excited-triplet state absorption and that of the slow decay residual. The results are shown in Figure 15, which reveals that the intensity of the excited-state absorption decreases with the increase in the excitation power, while the intensity of the slow residual decay shows the opposite trend. The dependence of the absorption intensity on the excitation power can be fitted by a second-order polynomial relation (the solid line).

Discussion

Interfacial Mass Transport. According to the multilayered model of an electrolyte solution at the interface of an electrode,[21] a diffusion layer is suggested to exist between the solid−liquid interface and the bulk solution. Taking the rotating disk electrode as an example, from the surface of the solid to the bulk solution, the multilayer consists of a compact (Stern) layer, diffuse layer, diffusion layer, and finally the hydrodynamical layer. The total thickness of the compact and the diffuse layers is approximately 1 to 10 nm,[22] while the diffusion layer depends on the hydrodynamics of the bulk solution. A well-stirred bulk solution has an accessible diffusion layer of about 10 μm in thickness,[21] whereas in a poorly stirred system, this value is about 100−200 μm.[23]

The thickness of the diffusion layer can be determined practically by direct[11−13] or indirect methods.[8,23,24] Here a brief introduction of the sonovoltammetry method is presented since it is more relevant to the present research. Sonovoltammetry employs ultrasound coupled to a heterogeneous electrochemical reaction at the electrode in solution phase, which enables the

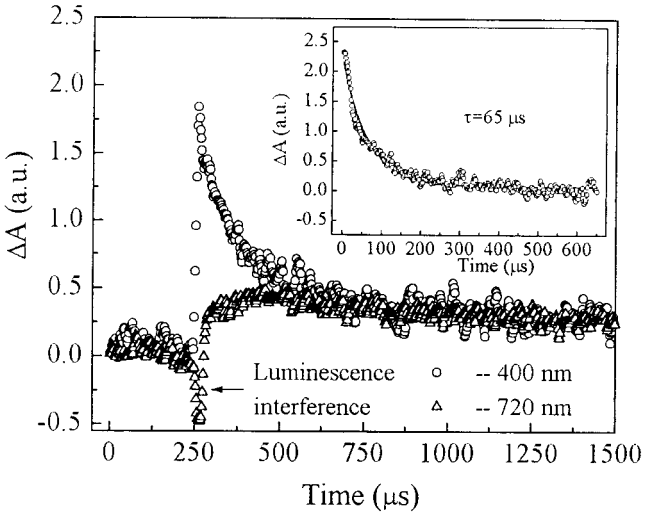

Figure 14. Kinetic decay traces for the transient absorption signals monitored at 400 and 720 nm, respectively, for a degassed acetonitrile solution of the complex Cu_6(t-NS)$_6$, $c = 1.0 \times 10^{-4}$ M, laser intensity: 6 mJ/pulse. Graphic inset: trace obtained by subtraction of 720 nm absorption from that of 400 nm (open circles). The solid line is the fitting curve of a monoexponential decay with a time constant of 65 μs.

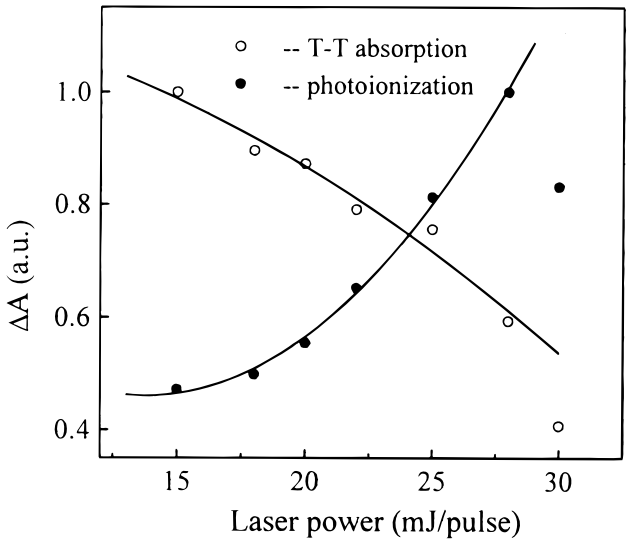

Figure 15. Plot of the absorption intensity for triplet−triplet transition and that of the slow decay component against the laser power in a 1.0 $\times 10^{-4}$ M degassed acetonitrile solution of Cu_6(t-NS)$_6$. (○): excited-triplet state absorption probed at 500 nm, acquired at 2 μs after the laser flash; biphotonic ionization (●) probed at 720 nm, acquired at 200 μs after the laser flash.

study of the ultrasonic effect on the double layer and the processes occurring therein.[24] Several possibilities of ultrasound affecting electrochemical reactions are identified as (1) the enhancement of mass transfer to and from electrode surface resulting from cavitation in solution, (2) continuous activation of the electrode surface, (3) the formation of ions, radicals, and other high-energy intermediates during transient cavitation, and (4) ultrasound enhancement of the rate of certain chemical reactions such as disproportions, coupled to the heterogeneous electron transfer.[25] In contrast to a general electrochemical cell, a sonoelectrochemical cell employs an additional ultrasonic horn close to the electrode. The ultrasonic power at the electrode can be varied by changing the distance between the ultrasonic horn and the electrode. It was found that greater ultrasonic power

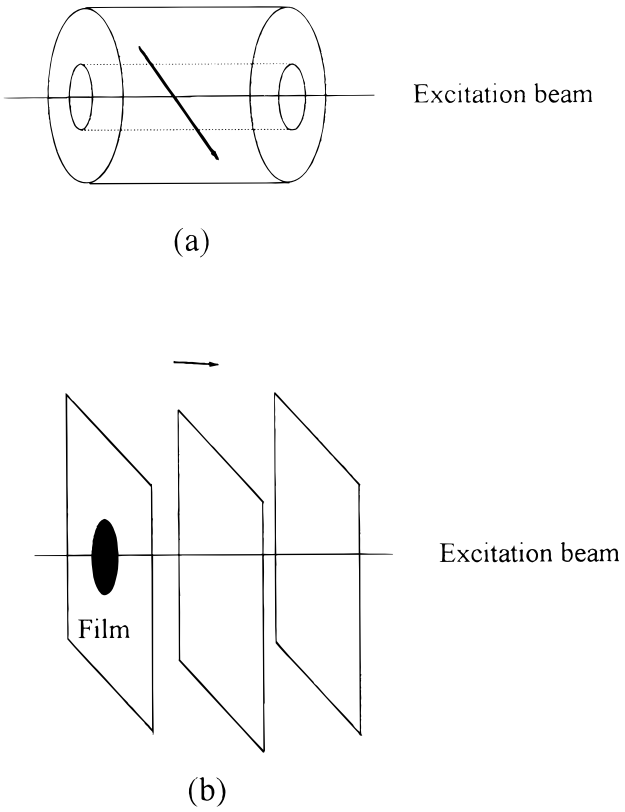

Figure 16. Schematic diagram showing the propagation of (a) cylindrical acoustic wave generated in the liquid phase by the thermal expansion of the illuminated volume; (b) plane acoustic wave generated by the light absorption of the metallic film deposition on the cell wall. The arrow indicates the propagating direction of the photoacoustic waves.

causes increased mass transport due to enhanced cavitation leading to a greater thinning of the diffusion layer. The estimated empirical correlation between the diffusion layer thickness (δ) and the ultrasonic power (p) is $\delta \propto p^{-0.6}$.[26]

In our flash photolysis experiment, the ultrasound can be generated at least via the following two mechanisms. (1) Weak cylindrical waves in a clean cell filled with a light absorbing medium: when a pulsed laser beam passes the light-absorbing medium, the thermal expansion of the illuminated volume generates cylindrical acoustic waves propagating in a lateral direction,[27] shown schematically in Figure 16a. (2) Intense plane wave in a cell deposited with metallic film: the metallic film absorbs the laser light producing thermal elastic waves due to the thermal expansion of the constrained thin film.[28,29] A substantial enhancement in strain-wave amplitude has been observed with an increase factor of ca. 100 over that from a transparent substrate.[30] In this case, the ultrasonic waves propagate along the excitation path, and the waveform depends on the focal size of the laser spot on the metallic film. In other words, when $\lambda/d \ll 1$ a plane wave is generated, while $\lambda/d \gg 1$ corresponds to a spherical wave, where λ is the wavelength of the acoustic wave and d is the diameter of the laser spot.[30] In our experiment, the excitation beam is defocused with a beam size of about 10 mm in diameter. This is sufficiently large to produce a reasonably collimated longitudinal MHz plane wave ($\lambda \sim 0.3$ mm for 1 MHz in the liquid) propagating along the excitation path. The generation and the propagation of the plane waves are shown schematically in Figure 16b.

As shown in Figure 1a, the onset of the transient absorbance change is clearly delayed by a period of time with respect to

the laser shot, which reveals that the observed signal is not from a primary photochemical reaction in the bulk solution, since the latter would give an instantaneous response. The delayed signal obviously indicates a secondary reaction which was retarded by most probably a physical process, for the delay time is dependent on the laser power (graphic inset in Figure 1b) and liquid volume (Figure 2). An intuitive explanation would be that the laser-generated active intermediates in the bulk solution cross the diffusion layer and undergo a subsequent interfacial reaction at the solid−liquid interface. The interfacial distinction of the reactions is evident from Figures 3 and 5. In Figure 3, the transient absorption signals were acquired for liquid films of different thickness coated on the cell wall. In terms of the multilayered structure model, trace 1 acquired for a thicker film can include the kinetics from both the adsorbed layer and the liquid continuum, while trace 2 for a thinner film reveals the reaction occurring most likely at the adsorbed layer. Therefore, the difference kinetic curve shown in trace 3 depicts the kinetics related to the liquid continuum. The kinetics of the adsorbed layer shows a monotonical decaying phase, while that of the liquid continuum exhibits a slow rising phase which is consistent to the scenarios that the photogenerated active species in the liquid continuum react at the solid surface via a slow diffusion process. The different kinetics for the delayed phase at different substrates (Figure 5) further reveals the interfacial distinction of the chemical reaction. Furthermore, comparing the kinetic trace detected in the perpendicular configuration of excitation and probe beams (Figure 1a) with that of overlapping configuration (Figure 4) for the bulk solution, it is obvious that in Figure 1a there is no observable early kinetics corresponding to the mass transfer process within the diffusion layer. Because in the perpendicular configuration the probe beam does not come across the interfaces exposed to the excitation beam, it is expected that there would be no photochemical reaction occurring within the diffusion layers being probed. This accounts for the absence of the transient absorption in the early kinetics in the former. The presence of the delayed phase in both normal and overlapping configurations of the excitation and probe beams is in agreement in that the diffusion process is indifferent to the configuration of the excitation and probe beams, while the delayed kinetics indicates that the photogenerated species in the bulk solution cross the diffusion layer before the interfacial reaction happens. It is known that the mass transfer in the bulk solution is greatly enhanced in the presence of the ultrasonic waves by acoustic streaming[31] cativation or micro-streaming,[32] which leads to a significant increase of the migration velocity in the bulk solution. Compared to the diffusion time taken in the diffusion layer, the time taken for the intermediate species migrating from the bulk solution to the diffusion layer would be negligible. The fact that the observed delay time is independent of the separation between the probed cell wall and the center of the excitation beam, the original source of the photogenerated species, indicates that the migration speed of the intermediate species in the bulk solution is much faster than that within the diffusion layer in the presence of the ultrasound. Therefore, the delay time is attributed to the time taken by the photogenerated species in the bulk solution crossing only the diffusion layer. Consequently the delay time can be a measure for the diffusion layer thickness.

It is expected that the diffusion time would be affected by the laser intensity, since the latter would change the concentration of the intermediate species in the bulk solution and the hydrodynamics of the liquid phase, hence the concentration gradient across the diffusion layer. It is found that at a fixed volume of solution, when the laser intensity is below 15 mJ/pulse, the diffusion time is kept nearly constant at 140 μs, while it decreases beyond 15 mJ/pulse, as shown in the inset of Figure 1b. It is known that chemical species reacting at the interface always have a steep concentration gradient across the diffusion layer.[33] According to the diffusion equation, a higher concentration gradient would lead to a larger effective driving force for the mass transport.[34] On the other hand, higher excitation power introduces a larger photoacoustic effect resulting in an enhanced mass-transfer, which also leads to a reduced value of the delay time. Consequently, the diffusion time would be reduced at high excitation power, and this can qualitatively account for the observed relationship between the delay time and the excitation power. In addition, Figure 2 shows that the diffusion time decreases with the decreasing liquid volume. It is known that the diffusion layer thickness depends on the hydrodynamics of the liquid which would be disturbed by the laser generated ultrasonic waves via stirring effect such as acoustic streaming, cativation, or microstreaming. At a given ultrasonic power (when the excitation power is fixed), the stirring efficiency would be inversely proportional to the liquid volume, resulting in a thicker diffusion layer at a larger filled liquid volume in the cell. Therefore the diffusion time is expected to decrease with the decrease of liquid volume. Assuming at a fixed laser power a fixed amount of ultrasonic energy is generated, and the ultrasonic power is defined as energy per volume, the diffusion layer thickness (δ) and the ultrasonic power (p) can be well correlated by $\delta \propto p^{-1}$, a relation comparable to that found in sonovoltammetry.[26]

Since the diffusion time can be directly measured in our experiment, and if the migration velocity of the species is known, the thickness of the diffusion layer can be evaluated straightforwardly. If the estimated value of the migration rate of active species is taken to be 0.114 cm/s,[35] and diffusion time is taken at the lower excitation power (140 μs), the thickness of the diffusion layer is estimated to be 0.2 μm. This estimated value can be compared to that obtained for the diffusion layer at an electrode in an electrochemical study from a recent publication, which reported an accessible diffusion layer thickness (in an aqueous solution) of 0.9 ± 0.3 μm using sonovoltammetric techniques.[36] It is also interesting to note the solvation of electrons generated by photoionization in aqueous micelle solution, where the electron has to travel outside the micelle into the bulk to get solvated, and the traveling distance can be a measure of the thickness of the micelle (several nm).[37,38] Note in Figure 2, when the filled liquid height, hence the liquid volume, approaches zero, which implies that the ultrasonic power becomes infinite, an intercept of 4.9 ± 1.7 μs is obtained (this value is taken from the intercept for a 1.0×1.0 cm cell; the deviation of the intercept for the 1.0×2.0 cm cell is too large) which corresponds to a layer thickness of 5.6 ± 1.9 nm. Physically at extremely high ultrasonic power, the diffusion layer approaches its lower limit where the separation between the bulk and the solid surface would be the thickness of the compact layer plus the diffuse layer, having a total thickness around 1∼10 nm.[22] Therefore, the intercept (5.6 ± 1.9 nm) can be a reasonable estimation for the thickness of these two layers.

Photochemical Reactions. The light sensitivity of Au(I) compounds is well documented,[39] and the reduction of Au(I) to metallic gold has been reported in the case of $Au(N_3)^-_2$.[40] In the present case, the dark gray film deposition on the cell wall is most likely due to the reduction of Au(I) to the metallic gold. Owing to the photodecomposition of the title complex, the detailed study for the photochemical reaction of an Au(I)

complex cannot be accomplished. However, the relative stability of the Cu_6(t-NS)$_6$ complex provides a possibility to explore the mechanism for the proceeding photochemical reactions as well as the interfacial process.

The Cu(I) complex has a hexanuclear Cu(I) core exhibiting metal−metal interaction. The emission spectrum has a large Stokes shift and can be assigned to the mixing effect of the excited triplet ^{3}LMCT (ligand-to-metal charge transfer) and ^{3}MCC (metal-cluster-centered) d → s transitions.[41] In addition to the absorption decay of the triplet-to-triplet transition, there is a long-lived residual component similar to a biphotonic ionization process reported for several organic and inorganic compounds shown in Figure 12.[42,43] Therefore, a biphotonic process can be a possible path for the undergoing photochemical reaction, which is further evidenced by the excitation power study of the photoproduct yields. As shown in Figure 15, the photoproduct yield of the triplet state decreases monotonically with the increased laser power beyond 15 mJ/pulse, while that for the residual decay absorption component shows a steady increase, except for the last two data points measured at 30 mJ/pulse. These two last data points indicate that significant photodecomposition occurs at higher excitation power. The quadratic dependence of the photoproduct yield for the residual decay component on the laser power suggests that a biphotonic process occurs.[42,44] The fact that the delayed phase can be quenched by dioxygen further suggests that the ionization is a consecutive biphotonic process,[44] i.e., the second photon is absorbed by the excited-triplet state. The energy for such a consecutive biphotonic excited state can be estimated from the onset of the emission spectrum E_{0-0} plus the energy of one excitation photon $h\nu$, resulting in a value of 5.4 eV; where E_{0-0} is estimated to be 1.9 eV (650 nm).

The ionization energy is not available for Cu_6(t-NS)$_6$; an ab initio calculated ionization energy of 7.9 eV is reported for the complex Cu_4(pyridine)$_4I_4$ in gas phase,[45] and it is taken as a close estimation for Cu_6(t-NS)$_6$. The difference between the ionization energy in gas phase and the consecutive biphotonic excitation in the liquid phase is 2.5 eV, which implies that only an effective solvation of the species generated by consecutive biphotonic light absorption can lead to a substantial ionization. The consecutive biphotonic light absorption of the Cu(I) complex would be expected to result in a charge separation pair. After sufficient solvation, the charge separation pair forms completely solvated cation and electron. At the solid−liquid interface, the solvated charge separation pair can be adsorbed, then further interact with the interface. Considering the static electric properties of the interface, the interaction between the adsorbed charge separation pair and the electrical field of the surface favors the full separation of the solvated charge separation pair into the corresponding solvated cation and electron. That the delayed phase decays faster at the glass substrate than at the quartz substrate reveals the different static electrical property of these two substrates, because the former contains cations such as Na^+, K^+, and the counteranions, etc. The consecutive biphotonic excitation and the subsequent ionization processes are summarized in the following scheme:

$$Cu_6(\text{t-NS})_6 + h\nu \rightarrow Cu_6(\text{t-NS})^*_6 \text{ (triplet state)} \quad (1)$$

$$Cu_6(\text{t-NS})^*_{6\ solv} + h\nu \rightarrow [Cu_6(\text{t-NS})_6^{+}\cdots e]_{solv} \text{ (charge separation pair)} \quad (2)$$

$$[Cu_6(\text{t-NS})_6^{+}\cdots e]_{solv} \rightleftharpoons Cu_6(\text{t-NS})_6^{+}{}_{solv} + e_{solv} \quad (3)$$

Surface adsorption and surface-assisted ionization:

$$[Cu_6(\text{t-NS})_6^{+}\cdots e]_{solv} \rightleftharpoons [Cu_6(\text{t-NS})_6^{+}\cdots e]_{ads} \quad (4)$$

$$[Cu_6(\text{t-NS})_6^{+}\cdots e]_{ads} \rightleftharpoons [Cu_6(\text{t-NS})_6]^{+}_{ads} + e_{ads} \quad (5)$$

where the subscripts "solv" and "ads" stand for the solvated and adsorbed species, respectively. The time-resolved difference absorption spectrum of Cu_6(t-NS)$_6$ (Figure 13) and the kinetics at different wavelengths (Figure 14) reveal that at least two intermediate species are generated in the biphotonic process, i.e., a faster decay species with peak absorption at 400 nm, and another much slower decay species generating the rest of the absorption spectrum. Figure 14 further shows that the two species follow different decay kinetics: one is of first-order decay, while the other is of second-order decay. According to the proposed scheme, the first-order decay can be assigned to the charge separation and the recombination process for the charge separation pair $[Cu_6(\text{t-NS})_6^{+}\cdots e]_{solv}$, whereas the charge recombination for $[Cu_6(\text{t-NS})_6]^+$ and the electron would follow second-order kinetics. Therefore, the absorption peak around 400 nm in Figure 14 is tentatively attributed to the charge separation pair $[Cu_6(\text{t-NS})_6^{+}\cdots e]_{solv}$ which has a lifetime of 65 μs. The much slower decay component with an absorption peaked at 460 and 800 nm in Figure 14 is tentatively assigned to the solvated cation $[Cu_6(\text{t-NS})_6]^+$ with a possible contribution from the solvated electron at the red side of the absorption spectrum. The slower decay component at 400 nm matches that at the other wavelengths (e.g., 720 nm in Figure 14) indicates that the equilibria described by eq 3−5 are maintained. As indicated in the above scheme, the interfacial reaction is the surface-assisted ionization of the solvated charge separation pair $[Cu_6(\text{t-NS})_6^{+}\cdots e]_{solv}$. To have a sufficient amount of $[Cu_6(\text{t-NS})_6^{+}\cdots e]_{solv}$ to arrive at the interface and undergo significant surface-assisted ionization, the charge separation pair must survive long enough to cross the diffusion layer. Since the absorption intensity of the delayed phase mainly comes from the solvated cation $[Cu_6(\text{t-NS})_6]^+$ and electron, which are long-lived species and in equilibrium with the charge separation pair, the absorbance of the delayed phase also reflects the concentration of the charge separation pair in the solution. Therefore, by measuring the delay time and the intensity of the delayed phase, a decay kinetics of the charge separation pair can be constructed as shown in Figure 10. Fitting the data points into a monoexponential decay equation gives a decay envelop with a lifetime of 65.4 μs (solid line), coincidental to the lifetime of the charge separation pair measured by the faster decay residual at 400 nm (65.0 μs). The consistency of the lifetime measurement by these two different methods strongly supports that the charge separation pair is the precursor for the successive interfacial chemical reaction. The dotted oscillation line in Figure 10 reflects the coupling between the interfacial chemical reaction and the photoacoustic waves.

Coupling of the Acoustic Wave with the Interfacial Chemical Reaction. *Chemical Process.* It has been reported that ultrasound can mediate a chemical process coupled to a heterogeneous electron transfer at the electrode, where the chemical process is accelerated in the presence of the ultrasound.[25] The effect of the ultrasonic mediation of a chemical process can also exist in our present flash photolysis study; however, its detailed mechanism cannot be identified at the moment.

In contrast to the prevailing mechanism for the coupling between ultrasonic effect and chemical reactions, where the ultrasonic waves act as an additional energy source in driving the reaction, here we suggest an alternative mechanism which

leads to the coupling between the acoustic effect and a heterogeneous chemical reaction resulting in the oscillation in the absorbance change.

An acoustic wave is basically a pressure wave generated by thermal expansion of the illuminated light absorbing medium. When pulsed laser is employed as an excitation source, a bipolar pressure pulse corresponding to the compression and rarefaction of the medium can be detected at a point in the medium away from the optical path;[46] therefore, an acoustic wave can be coupled to an interfacial chemical reaction as a pressure wave. When a pressure wave acts on the interface, the compression phase of the pressure wave leads to an increase in local concentration of $[Cu_6(t\text{-}NS)_6\cdots e]_{solv}$, which in turn causes equilibrium (4) to be right shifted. In response to such a change, a right shift in equilibrium (5) can be expected. Consequently, more cations $[Cu_6(t\text{-}NS)_6]^+_{ads}$ are generated, giving rise to an absorption peak on the transient absorption decay envelope, for the light absorption signal is mainly due to the longer-lived ionized species. On the other hand, the rarefaction phase would cause the local concentration to be less than that in the bulk, and shifts equilibrium (4) to the left, which produces a minimum on the transient absorption decay envelope. Therefore, the detected oscillation in absorbance change indicates the interaction of the acoustic wave on the solid−liquid interface. Though the probe beam detects the absorbance change contributed from both the interface and the bulk solution, the absorbance change due to the local concentration change in the bulk solution caused by the acoustic wave can hardly be detected, because the effects from the compression and rarefaction phase offset each other. Therefore only the adsorbed ionized species ($[Cu_6(t\text{-}NS)_6]^+_{ads}$, e_{ads}) at the interface can give a substantial contribution to the transient oscillations in response to the acoustic wave, while those in the bulk contribute only to the decaying envelope as shown in Figure 7. Because the acoustic wave generated by the light absorption of the liquid is a cylindrical wave propagating in a direction lateral to the excitation path, the coupled signal should depend on the method of arrangement of the excitation and probe beams. When the probe beam is arranged at a right angle to the excitation beam, the coupling signal can be detected; however, if the probe beam is parallel to the excitation path, the probe beam cannot reflect the acoustic wave propagation in the bulk. Figure 4 shows the absorption signal detected in an overlapping mode of excitation and probe beams compared to Figure 1, which is acquired in a normal configuration; the acoustic wave propagation process is apparently missing. The oscillation frequency of ultrasonic reflections in the first phase depending on the probing path length is also consistent with the ultrasound propagating along the probe beam. In the control experiment, where a clean cell is filled with a light absorbing medium, the absence of the transient absorption signal excludes the possibility that the oscillations come from a single physical process. Thus, the control experiment supports the conclusion that the observed oscillation in the clean cell is originated from the coupling between the acoustic wave and the chemical reactions. Analogous to the Cu(I) complex, this reaction scheme for the surface-assisted consecutive biphotonic ionization coupled to a pressure wave is believed to be valid for the Au(I) complex.

Physical Process. Generation of intense ultrasonic wave from metal−liquid interfaces has been reported.[29] Basically, the interface is constructed by a three-layered structure consisting of (1) a transparent substrate containing (2) an optically absorbing metallic film in contact with (3) a liquid. Generally the conversion efficiency from optical to thermoelastic power is low;[47] however, this construction can produce acoustic waves intense enough to be used in nondestructive ultrasonic detection. In our experiment, the metallic film developed on the inner surface of the cell acts just as an ultrasonic source when it absorbs the pulsed laser light. The generated plane acoustic wave propagates in the medium as a pressure wave, inducing a thermal refractive index gradient in the liquid along the excitation path. When the probe beam is arranged normal to the excitation path so as to the gradient of refractive index, similar to the experimental flow visualization described as the schlieren method,[48] the probe beam would be deflected from its undisturbed path, resulting in a modulation of the illumination intensity on the PMT, which finally gives an oscillation signal riding on the kinetic decay trace. Therefore, the beam deflection signal due to the schlieren effect reflects the acoustic wave propagation in the liquid medium. In a clean cell, the intensity of the acoustic wave is relatively much weaker and the effect of the beam deflection is not significant, as indicated by the control experiment. However, such an effect becomes obvious in a cell deposited with metallic film because the acoustic effect would be intensified by an order of 2 in magnitude over that in a clean cell, which gives rise to the observed ultrasonic reflection detected in the neat solvents. Therefore, this kind of oscillation is caused by a single physical process. As it is discussed above, the ultrasonic wave generated from the metal−liquid interface is a plane wave propagating along the excitation path, which accounts for the observed dependency of ultrasonic reflection period on the excitation path length in a cell deposited with metallic film and filled of the solvent only.

Conclusion

We confirmed that the UV pulsed laser induced photochemical reaction for $[\{Au[P(C_6H_4OMe\text{-}p)_3]\}_2\text{-}(\mu\text{-}C{\equiv}C)]$ is an interfacial process. A few hundred microseconds of delay time in the transient absorption signal after the laser flash are attributed to the mass-transfer of the photogenerated active species in the bulk solution crossing the diffusion layer, leading to a detectable interfacial chemical reaction at the solid−liquid interface. The delay time is suggested as a measure for the diffusion layer thickness. The thickness of the diffusion layer (0.2 μm) and that of the compact layer plus the diffuse layer (5.6 ± 1.9 nm) determined by this method is quite in agreement with the literature values considering the uncertainty of the migration rate of the active species.

Oscillations in the delayed phase are unambiguously determined to be originating from a chemical process by O_2 quenching experiment; however, the ultrasonic reflection signals appearing immediately after the laser flash can be from either a chemical process (i.e., coupling between an interfacial chemical reaction and the ultrasonic waves) or a single physical process (schlieren effect). Their origins can be distinguished by the oscillation frequency dependence on either probe path length (for the former) or the excitation path length (for the latter).

The photochemistry of complex $Cu_6(t\text{-}NS)_6$ which exhibits observed phenomena similar to that of the $[\{Au[P(C_6H_4OMe\text{-}p)_3]\}_2\text{-}(\mu\text{-}C{\equiv}C)]$ complex is studied by means of flash photolysis. The results show that the Cu(I) complex undergoes consecutive biphotonic ionization through an excited-triplet state. An intermediate species termed as charge separation pair having a light absorption maximum around 400 nm and a lifetime of 65 μs is generated during this process. An interfacial reaction mechanism involving the surface-assisted ionization is proposed to account for the coupling between the chemical reaction and the sound wave, which acts basically as a bipolar pressure wave.

According to this mechanism the intermediate species have to cross the diffusion layer to participate the interfacial reaction, and the decay kinetics of the intermediate species can be reconstructed by plot of the intensity of the delayed phase against the delay time, which leads to a lifetime of 65 μs, consistent to that from the direct measurement.

Our study provides a different aspect to understand the role of acoustic waves in the mass transfer process as well as the coupling between the heterogeneous reaction. Owing to the synchronization between the acoustic waves and the excitation laser shot and the interfacial sensitivity of the selected probe molecules, this method may have an additional advantage to study the fast dynamic process invoked by the acoustic effect with a microsecond or a better temporal resolution, depending on the pulse width of the laser and the resolution of the electronics.

Acknowledgment. We acknowledge the financial support from The University of Hong Kong, the Croucher Foundation, and the Hong Kong Research Grants Council.

References and Notes

(1) Turro, N. J.; Grätzel, M.; Braun, A. M. *Angew. Chem., Int. Ed. Engl*. **1980**, *19*, 675.
(2) Grätzel, M. *Heterogeneous Photochemical Electron Transfer*; CRC Press: Boca Raton, Florida, 1989.
(3) Kay, A.; Grätzel, M. *Solar Energy Mater. Solar Cells* **1996**, *44*, 99.
(4) Fendler, J. H. *Chem. Rev.* **1987**, *87*, 877.
(5) Compton, R. G.; Eklund, J. C.; Marken, F. *Electroanalysis* **1997**, *9*, 509.
(6) Akkermans, R. P.; Roberts, S. L.; Marken, F.; Coles, B. A.; Wilkins, S. J.; Cooper, J. A.; Woodhouse, K. E.; Compton, R. G. *J. Phys. Chem. B.* **1999**, *103*, 9987.
(7) Hagan C. R. S.; Coury, L. A., Jr. *Anal. Chem.* **1994**, *66*, 399.
(8) Klima, J.; Bernard, C.; Degrand, C. *J. Electroanal. Chem.* **1994**, *367*, 297.
(9) Compton, R. G.; Eklund, J. C.; Marke, F. *Electroanalysis* **1997**, *9*, 509.
(10) Compton, R. G.; Eklund, J. C.; Marken, F.; Rebbitt, T. O.; Akkermans, R. P.; Waller, D. N. *Electrochim. Acta* **1997**, *42*, 2919.
(11) Amatore, C.; Bonhomme, F.; Bruneel, J.-L.; Servant, L.; Thouin, L. *Electrochem. Commun*. **2000**, *2*, 235.
(12) Amatore, C.; Szunerits, S.; Thouin, L. *Electrochem. Commun*. **2000**, *2*, 248.
(13) Amatore, C.; Szunerits, S.; Thouin, L.; Warkocz, J. S. *Electrochem. Commun.* **2000**, *2*, 353.
(14) Weng, Y.-X.; Xiao, H.; Chan, K.-C.; Che, C.-M. *Chem. Phys. Lett.* **1997**, *270*, 315.
(15) Kitagawa, S.; Munakata, M.; Shimono, H.; Matsuyama, S.; Masuda, H. *J. Chem. Soc., Dalton Trans*. **1990**, 2105.
(16) Castro, R.; Duran, M. L.; Garcia-Vazquez, J. A.; Romero, J.; Sousa, A.; Castellano, E. E.; Zukerman-Schpector, J. *J. Chem. Soc., Dalton Trans*. **1992**, 2559.
(17) Kitagawa, S.; Kawata, S.; Nozaka, Y.; Munakata, M. J. *Chem. Soc. Dalton Trans*. **1993**, 1399.
(18) Cross, R. J.; Davidson, M. F. *J. Chem. Soc., Dalton Trans*. **1986**, 411.
(19) Xiao, H.; Cheung, K.-K.; Guo, C.-X.; Che, C.-M. *J. Chem. Soc., Dalton Trans.* **1994**, 1867.
(20) Weng, Y.-X.; Chan, K.-C.; Tzeng, B.-C.; Che, C.-M. *J. Chem. Phys.* **1998**, *109*, 5948.
(21) Albery, J. *Electrode Kinetics*; Clarenden Press: Oxford, 1975.
(22) Wu, H.; Li, Y. *Electrochemical Kinetics*; China Higher Education Press: Beijing, and Springer-Verlag: Berlin, Heidelberg, 1998; p 73.
(23) Gileadi, E. *Electrode Kinetics for Chemists, Chemical Engineers, and Materials Scientist*; VCH: New York, 1993; p 86.
(24) Marken, F.; Eklund, J. C.; Compton, R. G. *J. Electroanal. Chem.* **1995**, *395*, 335.
(25) Compton, R. G.; Eklund, J. C.; Page, S. D.; Rebbitt, T. O. *J. Chem. Soc., Dalton Trans*. **1995**, 389.
(26) Walton, D. J.; Phull, S. S.; Chyla, A.; Lorimer, J. P.; Mason, T. J. *J. Appl. Electrochem.* **1995**, *25*, 1083.
(27) (27) Patel, C. K. N.; Tam, A. C. *Rev. Mod. Phys.* **1981**, *53*, 517.
(28) Tam, A. C.; Leung, W. P. *Phys. Rev. Lett.* **1984**, *53*, 560.
(29) von Gutfeld, R. J.; Budd, H. F. *Appl. Phys. Lett.* **1979**, 34, 617.
(30) von Gutfeld, R. J.; Melcher, R. L. *Appl. Phys. Lett*. **1977**, *30*, 257.
(31) Nyborg, W. L. M. In *Physical Acoustics*, Mason, W. P., Ed.; Academic Press: New York, 1965; Vol. 2B, p 265.
(32) Leighton, T. G. *The Acoustic Bubble*; Academic Press: London, 1994; p 408ff.
(33) Marken, F.; Goldfarb, D. L.; Compton, R. G. *Electroanalysis* **1998**, *10*, 562.
(34) Page, C. H. *Physical Mathematics*; D. Van Nostrand: Princeton, N. J., 1955.
(35) Field, R. J.; Noyes, R. M. *Acc. Chem. Res*. **1977**, *10*, 214.
(36) Hill, H. A. O.; Nakagawa, Y.; Marken, F.; Compton, R. G. *J. Phys. Chem*. **1996**, *100*, 17395.
(37) Ghosh, H. N.; Palit, D. K.; Sapre, A. V.; RamaRao, K. V. S.; Mittal, J. P. *Chem. Phys. Lett*. **1993**, *203*, 5.
(38) Zoltewicz, J. A.; Bloom, L. B. *J. Phys. Chem*. **1992**, *96*, 5156.
(39) Kunkely, H.; Vogler, A. *Inorg. Chem*. **1992**, *31*, 4539.
(40) Vogler, A.; Quett, C.; Kunkely, H. *Ber. Bunsen-Ges., Phys. Chem.* **1988**, *92*, 1486.
(41) Sabin, F.; Ryu, C. K.; Ford, P. C.; Volger, A. *Inorg. Chem*. **1992**, *31*, 1941.
(42) Cho, K. C.; Che, C. M. *Chem. Phys. Lett.* **1986**, *124*, 313.
(43) Potashnik, R.; Ottolenghi, M.; Bensasson, R. *J. Phys. Chem*. **1969**, *73*, 1912.
(44) Lachish, U.; Shafferman, A.; Stein, G. *J. Chem. Phys*. **1976**, *64*, 4205.
(45) Vitale, M.; Palke, W. E.; Ford, P. C. *J. Phys. Chem*. **1992**, *96*, 8327.
(46) Tam, A. C.; Patel, C. K. N. *Applied Optics* **1979**, *18*, 3348.
(47) White, R. M. *J. Appl. Phys*. **1963**, *34*, 3559.
(48) Goldstein, S., Ed. *Modern Developments in Fluid Dynamics*; Clarendon Press: Oxford, 1957; Vol. I.